Available online at www.sciencedirect.com
SCIENCE DIRECT®
Journal of Sound and Vibration 276 (2004) 419–430
JOURNAL OF SOUND AND VIBRATION
www.elsevier.com/locate/jsvi

Letter to the Editor

Longitudinal vibrations of a double-rod system coupled by springs and dampers

H. Erol, M. Gürgöze*

Faculty of Mechanical Engineering, Technical University of Istanbul, 80191 Gümüşsuyu, Istanbul, Turkey

Received 20 May 2003; accepted 27 October 2003

1. Introduction

The study of the dynamical behavior of laterally vibrating double-beam systems has stimulated the interest of researchers [1–3]. In the interesting study [3] published in this journal, an exact method was presented for solving the vibration of a double-beam system subjected to harmonic excitation. The system has a main beam with an applied force, and an auxiliary beam with a distributed spring k and damper c in parallel between the two beams. Motivated by this publication, the present paper deals with longitudinally vibrating double-rod systems as a counterpart of that publication. This paper presents a method of obtaining the exact solution for the forced vibrations of elastic rods coupled by distributed springs and dampers. The method is based on the change of variables to decouple the set of two second order partial differential equations, and then the solutions are obtained by means of modal analysis. The two restrictions made are that the rods must be identical, and the boundary conditions on the same side of the system must be the same. In order to demonstrate the method in detail, a case study is chosen; the two rods are fixed-free supported and the forcing function is a concentrated axial sinusoidal load applied at the midpoint of the primary rod. The complete solutions are derived, and frequency responses are plotted for various values of stiffness and damping.

2. Theory

The problem to be dealt with in the present study is the forced vibration problem of the system shown in Fig. 1. It consists of two fixed-free axially vibrating elastic rods to which a distributed spring-damper system, as a model of a viscoelastic material is attached across the span. The primary rod is assumed to be subjected to a distributed forcing function $f(x,t)$. A secondary rod is connected to the primary rod by a viscoelastic material. This material is modelled as a distributed

*Corresponding author. Fax: +90-212-245-07-95.
E-mail address: gurgozem@itu.edu.tr (M. Gürgöze).

0022-460X/$ - see front matter
doi:10.1016/j.jsv.2003.10.043

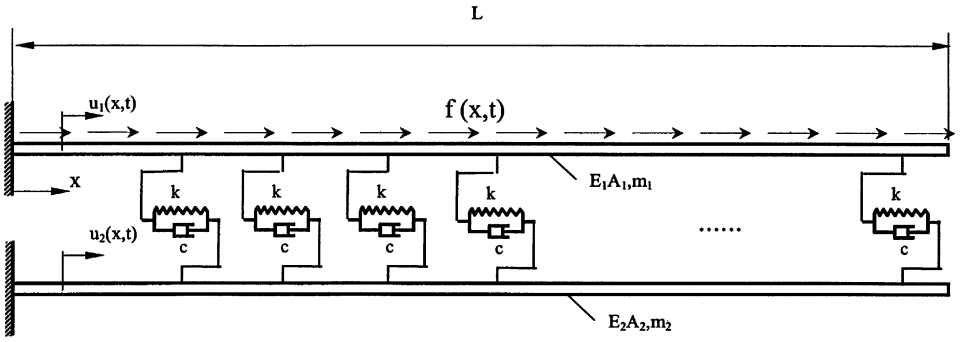

Fig. 1. Longitudinally vibrating elastic rods coupled by distributed springs and dampers.

spring-damper system, where k and c are the spring constant and the damping coefficient, respectively. In general, the two rods are different where the length, mass per unit length and axial rigidity of the ith rod are L_i, m_i and E_iA_i $(i = 1, 2)$, respectively. These parameters are assumed to be constant along each rod. The longitudinal displacements over the two rods are denoted by $u_1(x, t)$ and $u_2(x, t)$, respectively.

The longitudinal vibration equations of the system are

$$-E_1A_1u_1''(x,t) + c[\dot{u}_1(x,t) - \dot{u}_2(x,t)] + k[u_1(x,t) - u_2(x,t)] + m_1\ddot{u}_1(x,t) = f(x,t), \tag{1}$$

$$-E_2A_2u_2''(x,t) - c[\dot{u}_1(x,t) - \dot{u}_2(x,t)] - k[u_1(x,t) - u_2(x,t)] + m_2\ddot{u}_2(x,t) = 0, \tag{2}$$

where x is the axial position along the rods. Dots and primes denote partial derivatives with respect to time t and position coordinate x, respectively. With a simple manipulation of variables, the equations can be uncoupled and modal analysis can be used to determine the solutions as in Ref. [3]. Let it be assumed that the boundary conditions are identical on each side of both rods and

$$E_1A_1 = E_2A_2 = e = \text{constant}, \quad m_1 = m_2 = m = \text{constant}, \tag{3}$$

where e and m denote the axial rigidity and mass per unit length, respectively. With the assumptions (3), Eqs. (1) and (2) become

$$-e\,u_1''(x,t) + c[\dot{u}_1(x,t) - \dot{u}_2(x,t)] + k[u_1(x,t) - u_2(x,t)] + m\ddot{u}_1(x,t) = f(x,t), \tag{4}$$

$$-e\,u_2''(x,t) - c[\dot{u}_1(x,t) - \dot{u}_2(x,t)] - k[u_1(x,t) - u_2(x,t)] + m\ddot{u}_2(x,t) = 0. \tag{5}$$

Assume that

$$u(x,t) = u_1(x,t) - u_2(x,t), \tag{6}$$

such that

$$u_1(x,t) = u(x,t) + u_2(x,t), \tag{7}$$

where $u(x, t)$ is the relative displacement of the primary rod with respect to the secondary rod. Use of the definition (6) yields for the difference of Eqs. (4) and (5) the following results:

$$-e\,u(x,t)'' + 2c\,\dot{u}(x,t) + 2k\,u(x,t) + m\ddot{u}(x,t) = f(x,t), \tag{8}$$

$$-e\,u_2''(x,t) + m\,\ddot{u}_2(x,t) = c\,\dot{u}(x,t) + k\,u(x,t). \tag{9}$$

For the solution of the above differential equations; first, Eq. (8) will be solved for the relative displacement $u(x,t)$. Then, Eq. (9) can be solved for the displacements of the secondary rod $u_2(x,t)$. Finally, Eq. (7) yields the displacement of the primary rod $u_1(x,t)$. Additionally, modal analysis will be employed for the solutions. With this procedure, the natural frequencies and the corresponding mode shapes will be obtained by solving the undamped free vibration equation with appropriate boundary conditions. Then, the orthonormality property is established. Finally, the forced vibration problem is solved by means of modal expansion.

In order to show the solution method in detail, similar to Ref. [3], the following case is considered: Both rods are fixed-free supported and the forcing function is a concentrated axial sinusoidal load applied at the midpoint of the primary rod. For this system, the boundary conditions are

$$\begin{aligned} &u_1(0,t) = 0, \quad eu_1'(L,t) = 0,\\ &u_2(0,t) = 0, \quad eu_2'(L,t) = 0. \end{aligned} \tag{10}$$

The forcing function can be represented as

$$f(x,t) = F(x)\cos\omega t = P\,\delta\left(x - \frac{L}{2}\right)\cos\omega t, \tag{11}$$

where P is constant, δ is the Dirac delta function and ω is the forcing frequency.

For undamped free vibrations, Eq. (8) becomes

$$-e\,u(x,t)'' + 2k\,u(x,t) + m\ddot{u}(x,t) = 0. \tag{12}$$

With Eq. (6), the boundary conditions associated with Eq. (12) are

$$\begin{aligned} &u(0,t) = u_1(0,t) - u_2(0,t) = 0,\\ &eu'(L,t) = eu_1'(L,t) - eu_2'(L,t) = 0. \end{aligned} \tag{13}$$

Assuming that the relative motion, $u(x,t)$ is in one of its natural modes of vibration, the solution of Eq. (12) is in the form

$$u(x,t) = U(x)\cos\omega t, \tag{14}$$

where ω is a natural frequency and $U(x)$ is the corresponding mode shape. Substituting Eq. (14) into Eq. (12), it follows that

$$U(x)'' + \lambda^2 U(x) = 0, \tag{15}$$

where

$$\lambda^2 = \frac{m\omega^2 - 2k}{e}, \tag{16}$$

is introduced.

Now the solution of Eq. (15) can be given as

$$u(x) = A\cos\lambda x + B\sin\lambda x. \tag{17}$$

The boundary conditions from Eq. (13) yield

$$U(0) = 0, \quad U'(L) = 0. \tag{18}$$

Thus, the frequency equation is

$$\cos \lambda L = 0, \tag{19}$$

and its roots are

$$\lambda_r L = (2r-1)\frac{\pi}{2} \quad (r = 1, 2, \ldots). \tag{20}$$

Comparison of Eqs. (16) and (20) gives

$$\sqrt{\frac{m\omega^2 - 2k}{e}} = (2r-1)\frac{\pi}{2L} \quad (r = 1, 2, \ldots). \tag{21}$$

Hence, the natural frequencies are

$$\omega_r = \sqrt{\left(\frac{(2r-1)\pi}{2L}\right)^2 \frac{e}{m} + \frac{2k}{m}} \quad (r = 1, 2, \ldots), \tag{22}$$

and the corresponding mode shapes are

$$U_r(x) = B_r \sin \lambda_r x = B_r \sin \frac{(2r-1)\pi}{2L} x \quad (r = 1, 2, \ldots). \tag{23}$$

If the mode shapes are normalized according to

$$\int_0^L m U_r^2(x)\, dx = 1 \quad (r = 1, 2, \ldots), \tag{24}$$

then

$$B_r = \sqrt{\frac{2}{mL}} \quad (r = 1, 2, \ldots), \tag{25}$$

is obtained, giving

$$U_r(x) = \sqrt{\frac{2}{mL}} \sin \frac{(2r-1)\pi}{2L} x \quad (r = 1, 2, \ldots). \tag{26}$$

Thus, the eigenfunctions satisfy the orthonormality property

$$\int_0^L m U_r(x) U_s(x)\, \mathrm{d}x = \delta_{rs}, \tag{27}$$

where δ_{rs} is the Kronecker delta.

A solution of Eq. (8) is assumed to be in the form

$$u(x, t) = \sum_{r=1}^{\infty} U_r(x) q_r(t), \tag{28}$$

where $U_r(x)$ is the rth mode shape and $q_r(t)$ is the corresponding generalized *coordinate* to be determined. Substituting Eq. (28) into Eq. (8) yields

$$\sum_{r=1}^{\infty} \left\{[-eU_r''(x) + 2kU_r(x)]q_r(t) + 2cU_r(x)\dot{q}_r(t) + mU_r(x)\ddot{q}_r(t)\right\} = f(x,t). \tag{29}$$

If Eq. (15) for $U(x) = U_r(x)$ together with Eq. (16) for $\lambda = \lambda_r$ is introduced into Eq. (29), it follows

$$\sum_{r=1}^{\infty}[m\ddot{q}_r + 2c\dot{q}_r + m\,\omega_r^2 q_r]U_r(x) = f(x,t). \tag{30}$$

Multiplying Eq. (30) by $U_s(x)$ and then integrating from $x = 0$ to L and making use of the property (27) yields

$$\ddot{q}_s(t) + 2\xi_s\omega_s\,\dot{q}_s(t) + \omega_s^2 q_s(t) = Q_s(t) \quad (s = 1, 2, \ldots) \tag{31}$$

where the sth generalized force is given by

$$Q_s(t) = \int_0^L f(x,t)U_s(x)\,\mathrm{d}x, \tag{32}$$

and the damping ratio is defined as

$$\xi_s = \frac{c}{m\omega_s}. \tag{33}$$

If the forcing function (11) and the mode function (26) are introduced into Eq. (32), it follows that

$$Q_s(t) = \sqrt{\frac{2}{mL}}P\cos\omega t\int_0^L \delta\left(x - \frac{L}{2}\right)\sin\frac{(2s-1)\pi}{2L}x\,\mathrm{d}x \quad (s = 1, 2, \ldots) \tag{34}$$

giving after some rearrangements:

$$Q_s(t) = \sqrt{\frac{1}{mL}}P\left(\sin\frac{s\pi}{2} - \cos\frac{s\pi}{2}\right)\cos\omega t \quad (s = 1, 2, \ldots). \tag{35}$$

Introducing Eq. (35) back into Eq. (31) gives

$$\ddot{q}_s(t) + 2\xi_s\omega_s\dot{q}_s(t) + \omega_s^2 q_s(t) = \sqrt{\frac{1}{mL}}P\left(\sin\frac{s\pi}{2} - \cos\frac{s\pi}{2}\right)\cos\omega\,t \quad (s = 1, 2, \ldots). \tag{36}$$

The steady state solution of Eq. (36) is

$$q_s(t) = \sqrt{\frac{1}{mL}}\frac{P}{\omega_s^2}\frac{\sin\dfrac{s\pi}{2} - \cos\dfrac{s\pi}{2}}{\sqrt{\left(1 - \dfrac{\omega}{\omega_s}\right)^2 + \left(2\xi_s\dfrac{\omega}{\omega_s}\right)^2}}\cos(\omega t + \theta_s) \quad (s = 1, 2, \ldots), \tag{37}$$

where

$$\theta_s(t) = -\tan^{-1}\left(\frac{2\xi_s\dfrac{\omega}{\omega_s}}{1 - \left(\dfrac{\omega}{\omega_s}\right)^2}\right) \quad (s = 1, 2, \ldots). \tag{38}$$

Introducing the mode function (26) and the time function (37) into Eq. (28), it follows:

$$u(x,t)=\sum_{r=1}^{\infty} A_r \sin\frac{(2r-1)\pi}{2L}\,x\cos(\omega t+\theta_r), \tag{39}$$

where

$$A_r=\frac{\sqrt{2}P\left(\sin\dfrac{r\pi}{2}-\cos\dfrac{r\pi}{2}\right)}{mL\omega_r^2\sqrt{\left(1-\dfrac{\omega}{\omega_r}\right)^2+\left(2\xi_r\dfrac{\omega}{\omega_r}\right)^2}} \quad (r=1,2,\ldots). \tag{40}$$

Now, $u_2(x,t)$ can be solved for. From Eq. (9), the forcing function of $u_2(x,t)$ is obtained as

$$f_2(x,t)=c\,\dot{u}(x,t)+k\,u(x,t). \tag{41}$$

Introducing Eq. (39) into Eq. (41) yields

$$f_2(x,t)=\sum_{r=1}^{\infty} A_r\sin\frac{(2r-1)\pi}{2L}\,x[k\cos(\omega t+\theta_r)-c\omega\sin(\omega t+\theta_r)], \tag{42}$$

which can be simplified to

$$f_2(x,t)=\sum_{r=1}^{\infty} A_r\sqrt{k^2+c^2\omega^2}\sin\frac{(2r-1)\pi}{2L}\,x\cos(\omega t+\theta_r+\varphi), \tag{43}$$

where

$$\varphi=\tan^{-1}\frac{c\omega}{k}. \tag{44}$$

Once again, modal analysis is employed to solve Eq. (9). The eigenvalues of the fixed-free elastic rod are

$$\lambda_{2r}^2=\frac{m\omega_{2r}^2}{e}=\left[\frac{(2r-1)\pi}{2L}\right]^2 \quad (r=1,2,\ldots), \tag{45}$$

where the subscript $2r$ denotes the rth mode of secondary rod. The natural frequencies are

$$\omega_{2r}=\sqrt{\left(\frac{(2r-1)\pi}{2L}\right)^2\frac{e}{m}} \quad (r=1,2,\ldots), \tag{46}$$

and the corresponding normalized mode shapes are

$$U_{2r}(x)=\sqrt{\frac{2}{mL}}\sin\frac{(2r-1)\pi}{2L}\,x \quad (r=1,2,\ldots). \tag{47}$$

The orthonormality property is given by

$$\int_0^L mU_{2r}(x)U_{2s}(x)\,\mathrm{d}x=\delta_{rs}. \tag{48}$$

If the solution of Eq. (9) is assumed in a series form

$$u_2(x,t) = \sum_{s=1}^{\infty} U_{2s}(x) q_{2s}(t), \tag{49}$$

$$\ddot{q}_{2s}(t) + \omega_{2s}^2 q_{2s}(t) = Q_{2s}(t). \tag{50}$$

is obtained where the corresponding generalized force is defined as

$$Q_{2s}(t) = \int_0^L f_2(x,t) U_{2s}(x)\,\mathrm{d}x \quad (s = 1,2,\ldots). \tag{51}$$

Introducing Eqs. (43) and (47) into Eq. (51) yields,

$$Q_{2s}(t) = \int_0^L \sqrt{\frac{2}{mL}} \sin\frac{(2s-1)\pi}{2L} x \times \left\{ \sum_{r=1}^{\infty} A_r \sqrt{k^2 + c^2\omega^2}\, \sin\frac{(2r-1)\pi}{2L} x \cos(\omega t + \theta_r + \varphi) \right\} \mathrm{d}x, \tag{52}$$

or after rearrangement:

$$Q_{2s}(t) = \left[\sum_{r=1}^{\infty} A_r \sqrt{k^2 + c^2\omega^2} \cos(\omega t + \theta_r + \varphi) \sqrt{\frac{L}{2m}} \right] \times \int_0^L m \sqrt{\frac{2}{mL}} \sin\frac{(2r-1)\pi}{2L} x \sqrt{\frac{2}{mL}} \sin\frac{(2s-1)\pi}{2L} x\,\mathrm{d}x. \tag{53}$$

Since the last integral in Eq. (53) is equal to the normalized orthogonality expression (48), all terms in the infinite series vanish except $r = s$. Hence,

$$Q_{2s}(t) = \sqrt{\frac{L}{2m}} A_s \sqrt{k^2 + c^2\omega^2} \cos(\omega t + \theta_s + \varphi) \quad (s = 1,2,\ldots). \tag{54}$$

is obtained. With Eq. (54), the steady state solution of Eq. (50) is

$$q_{2s}(t) = \frac{\sqrt{\frac{L}{2m}} A_s \frac{\sqrt{k^2 + c^2\omega^2}}{\omega_{2s}^2}}{1 - \left(\frac{\omega}{\omega_{2s}}\right)^2} \cos(\omega t + \theta_s + \varphi) \quad (s = 1,2,\ldots). \tag{55}$$

After substituting the mode function (47) and the generalized coordinate (55) into Eq. (49), the steady state solution of Eq. (9) is obtained as

$$u_2(x,t) = \sum_{r=1}^{\infty} \frac{1}{m\omega_{2r}^2} \frac{A_r \sqrt{k^2 + c^2\omega^2}}{1 - \left(\frac{\omega}{\omega_{2r}}\right)^2} \sin\frac{(2r-1)\pi}{2L} x \cos(\omega t + \theta_r + \varphi) \quad (r = 1,2,\ldots). \tag{56}$$

Finally, the steady state solution of the primary rod is determined by Eq. (7):

$$u_1(x,t) = u(x,t) - u_2(x,t).$$

3. Numerical evaluations

This section is devoted to the numerical evaluation of the expressions obtained above. For the numerical applications, values in Table 1 are chosen for the physical data of the mechanical system in Fig. 1. Additionally, frequency responses are obtained for low and high values of stiffness ($k = 10,\ 800$ N/m) and damping ($c = 0, 0.2$ kg/s).

The first six natural frequencies of the system are given in Table 2 for systems with low and high stiffness values. It is worth noting that only the first of the pairs of natural frequencies of each mode r is independent of the stiffness k.

The frequency responses at the mid-point in the span of the rods are shown in Figs. 2–7. The mid-point of the span of the rods is chosen because of symmetry of the rod system and the location of applied load. Additionally, frequency responses are rearranged as a logarithmic expression in order to compare to the results in the reference study [3] being under the assumption that $U_o = 0.001$.

Fig. 2 shows the absolute amplitudes of the primary rod at the mid-span for low ($k = 8$ N/m) and high stiffness ($k = 80$ N/m) values, with and without damping ($c = 0.2$ kg/s). Fig. 3 represents amplitudes of the secondary rod at the mid-point in the span for low ($k = 8$ N/m) and high stiffness values, with and without damping ($c = 0.2$ kg/s).

Table 1
Values of the physical parameters of the rods

L (m)	1
m (kg/m)	1
e (N/m^2)	1
P (N)	0.001

Table 2
First six natural frequencies of the systems with low and high stiffness values

r	Stiffness k (N/m)	
	8	80
1	1.5708	1.5708
	4.2974	12.7463
2	4.7124	4.7124
	6.1812	13.4984
3	7.8540	7.8540
	8.8139	14.8891

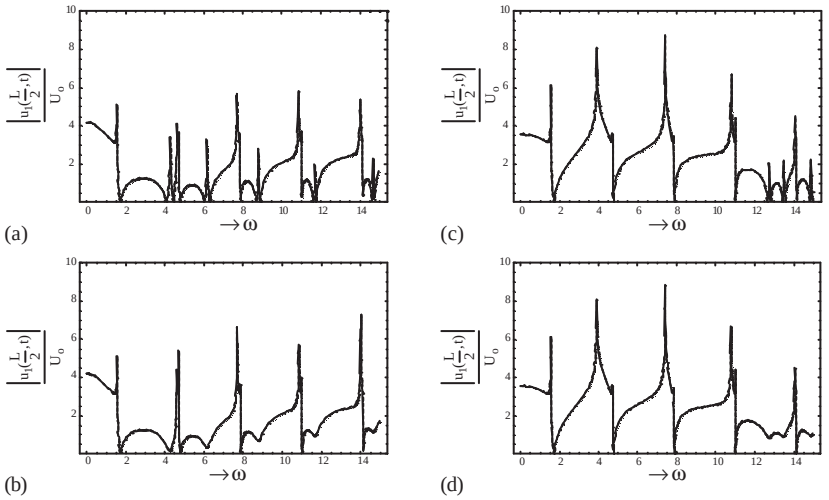

Fig. 2. Absolute amplitudes of the primary rod at the mid-span for (a) $k = 8$ N/m, $c = 0$; (b) $k = 8$ N/m, $c = 0.2$ kg/s; (c) $k = 80$ N/m, $c = 0$ and (d) $k = 80$ N/m, $c = 0.2$ kg/s.

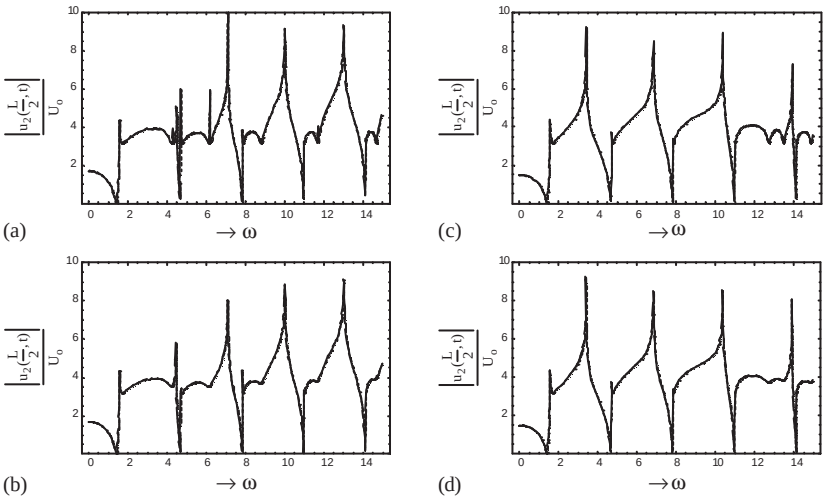

Fig. 3. Absolute amplitudes of the secondary rod at the mid-span for (a) $k = 8$ N/m, $c = 0$; (b) $k = 8$ N/m, $c = 0.2$ kg/s; (c) $k = 80$ N/m, $c = 0$ and (d) $k = 80$ N/m, $c = 0.2$ kg/s.

Comparisons of the plots represented in Figs. 2 and 3 show that the first of the pairs of natural frequencies of each mode r demonstrated in Table 2 are unaffected by damping. Damping suppresses only the resonance peaks corresponding to the second of the pairs of natural frequencies of each mode r demonstrated. The effects of stiffness on the natural frequencies and corresponding resonances are such that the natural frequencies separate from one another and the resonance peaks are growing up.

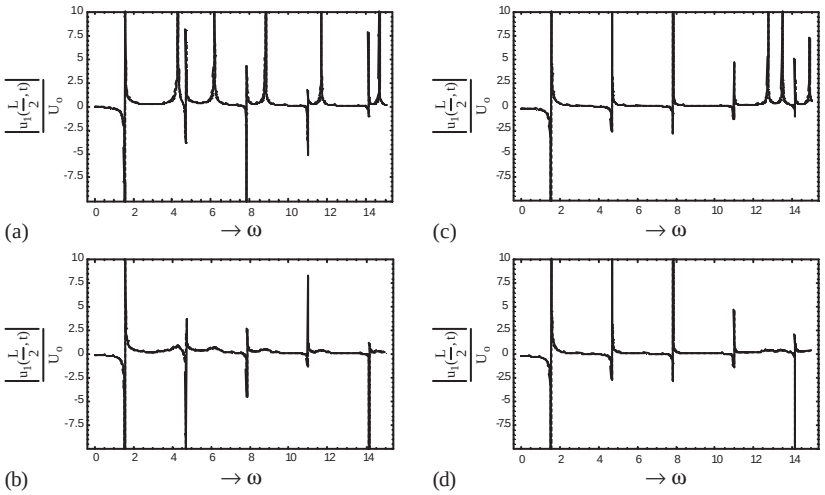

Fig. 4. Amplitudes of the primary rod at the mid-span for (a) $k = 8$ N/m, $c = 0$; (b) $k = 8$ N/m, $c = 0.2$ kg/s; (c) $k = 80$ N/m, $c = 0$ and (d) $k = 80$ N/m, $c = 0.2$ kg/s.

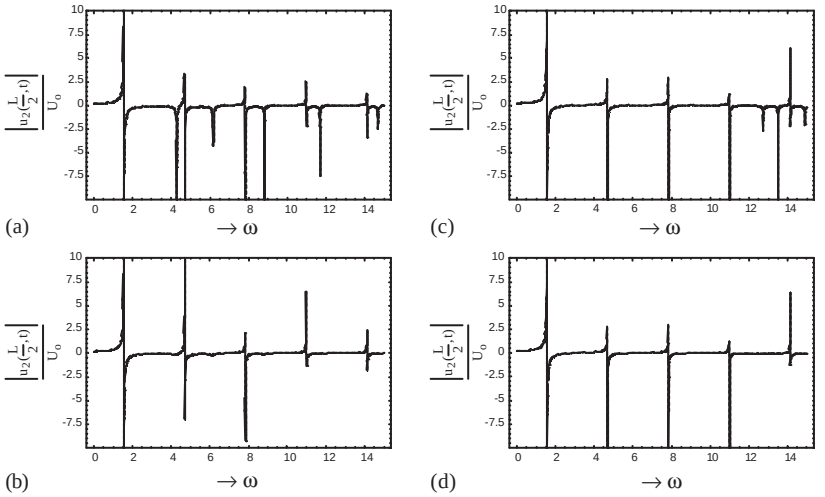

Fig. 5. Amplitudes of the secondary rod at the mid-span for (a) $k = 8$ N/m, $c = 0$; (b) $k = 8$ N/m, $c = 0.2$ kg/s; (c) $k = 80$ N/m, $c = 0$ and (d) $k = 80$ N/m, $c = 0.2$ kg/s.

Fig. 4 illustrates the absolute amplitude of the primary rod at the mid-span for low ($k = 8$ N/m) and high stiffness ($k = 80$ N/m) values, with and without damping ($c = 0.2$ kg/s). Fig. 5 shows amplitudes of the secondary rod at the mid-point in the span for low ($k = 8$ N/m) and high stiffness values, with and without damping ($c = 0.2$ kg/s).

Comparisons of the plots represented in Figs. 4 and 5 clarify that the first of the pairs of natural frequencies of each mode r demonstrated in Table 2 are unaffected by damping. Damping suppresses only the resonance peaks corresponding to the second of the pairs of natural

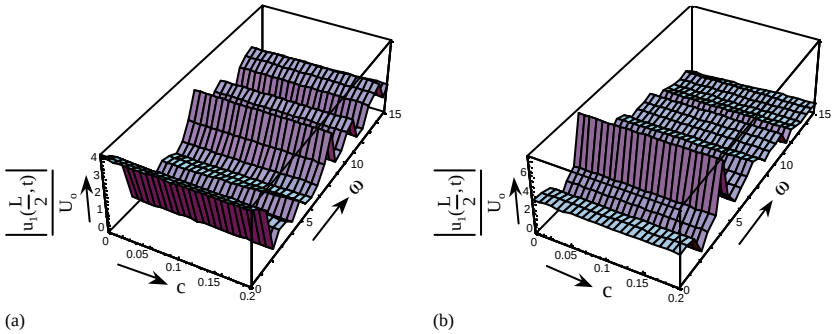

Fig. 6. Three-dimensional plots of the frequency responses of the primary rod with varying damping for (a) $k = 8$ N/m and (b) $k = 80$ N/m.

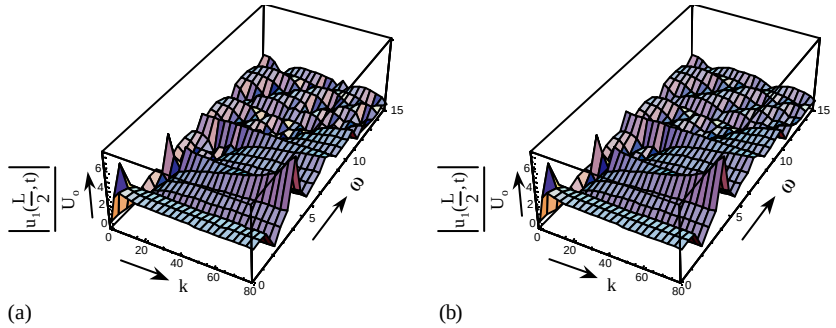

Fig. 7. Three-dimensional plots of the frequency responses of the primary rod with varying stiffness values for (a) $c = 0$ and (b) $c = 0.2$ kg/s.

frequencies of each mode r demonstrated which is the same as the primary rod. The effects of stiffness on the natural frequencies and corresponding resonances are such that the natural frequencies separate from one another as seen in the primary rod and there is no significant change in the resonance peaks in this rod.

Fig. 6 illustrates the three-dimensional plots of the frequency responses of the primary rod with varying damping for low ($k = 8$ N/m) and high stiffness ($k = 80$ N/m) values. This figure clarifies that the damping suppresses only the resonance peaks corresponding to the second of the pairs of natural frequencies of each mode r demonstrated in Table 2.

Fig. 7 represents the three-dimensional plots of the frequency responses of the primary rod with varying stiffness values for undamped and damped cases ($c = 0.2$ kg/s). This figure strengthens the above outcomes.

Fig. 8 shows the three-dimensional plots of the amplitudes at various points along both rods, for undamped and high stiffness values ($k = 80$ N/m). These figures show that the rods follow their own dominant natural modes. Furthermore, the rods vibrate in-phase at the first of the pairs of natural frequencies of each mode r demonstrated in Table 2 and out-of-phase at the second of the pairs of natural frequencies.

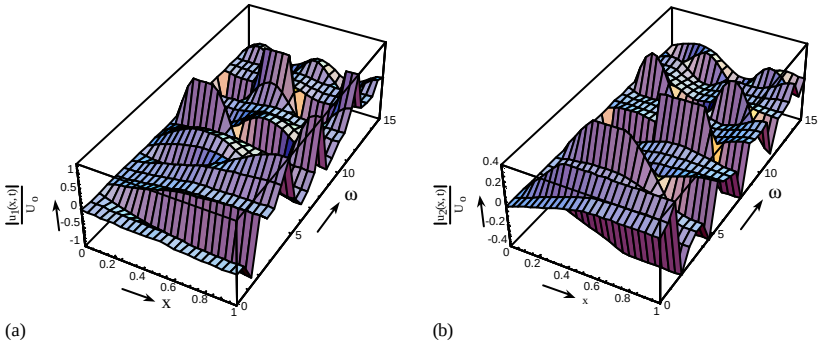

Fig. 8. Three-dimensional plots of the amplitudes at various points along the both rods, for $k = 80$ N/m, $c = 0$, (a) primary rod and (b) secondary rod.

Since damping does not affect the in-phase modes of an identical rod system, the secondary rod cannot be used effectively over a wide range of frequencies as a distributed dynamic vibration absorber for the primary rod.

4. Conclusions

This study is concerned with the establishment of a closed form solution for longitudinally vibrating elastic rods coupled by distributed springs and dampers. The method is based on the change of variables to decouple the set of two second order partial differential equations, and then the solutions are obtained by means of modal analysis. The damping need not be small or proportional to the mass and stiffness, which is different to the conventional methods, and the forcing function can either be distributed or concentrated at any point. The two restrictions of this method are that the rods must be identical, and the boundary conditions on the same side of the system must be the same. The plots show that each natural mode has two submodes. One is the in-phase submode whose natural frequencies are independent of stiffness and damping. Another is the out-of-phase submode whose natural frequencies are increased with increasing stiffness and resonant peaks are decreased with increasing damping. Although it is acknowledged that the presented method is applicable only for a limited class of problems, it provides an analytical solution that can serve as a benchmark for further investigation of more complex n-rod systems.

References

[1] M. Gürgöze, G. Erdoğan, S. İnceoğlu, Bending vibrations of beams coupled by a double spring-mass system, *Journal of Sound and Vibration* 243 (2001) 361–369.

[2] S. İnceoğlu, M. Gürgöze, Bending vibrations of beams coupled by several double spring-mass systems, *Journal of Sound and Vibration* 243 (2001) 370–379.

[3] H.V. Vu, A.M. Ordonez, B.H. Karnopp, Vibration of a double-beam system, *Journal of Sound and Vibration* 229 (2000) 807–822.